

# Ultrasound Elastography Detects Age-Related Changes in Adult False Vocal Folds

Lucas Chandra, BS, Julian Ortiz, MS, William Weitzel, MD, James D. Hamilton, PhD, Jing Gao, MD 

Received March 19, 2022, from the Rocky Vista University, Ivins, UT, USA (L.C., J.O., J.G.); VA Ann Arbor Healthcare System, Ann Arbor, MI, USA (W.W., J.D.H.); University of Michigan, Ann Arbor, MI, USA (W.W., J.D.H.); and Weill Cornell Medicine, Cornell University, New York, NY, USA (J.G.). Manuscript accepted for publication May 15, 2022.

We thank Siemens Healthineers for cosigned equipment to support the study.

Address correspondence to Jing Gao, MD, Director of Ultrasound in Research and Education, Rocky Vista University, 255 E. Center Street, Ivins, UT 84738, USA.

E-mail: [jgao@rvu.edu](mailto:jgao@rvu.edu)

## Abbreviations

ARFI, acoustic radiation force impulse; DICOM, Digital Imaging and Communications in Medicine; FVF, false vocal fold; ICC, intraclass correlation coefficient; SWE, shear wave elastography; SWV, shear wave velocity; VTIQ, Virtual Touch Tissue Quantification

doi:10.1002/jum.16033

**Purpose**—To investigate the feasibility of ultrasound elastography for assessing the symmetry in stiffness values and movements of both false vocal folds (FVFs).

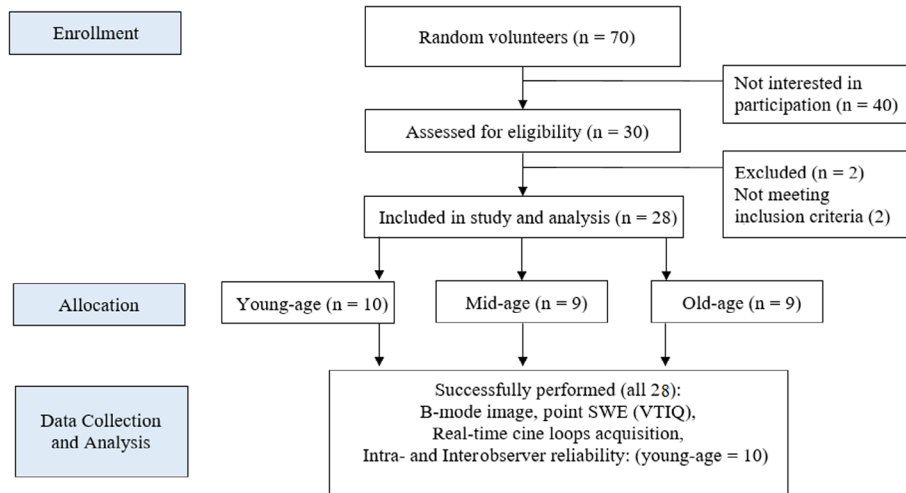
**Methods**—After Institutional Review Board's approval and written informed consent obtained, we measured ultrasound strain and shear wave velocity (SWV) of the bilateral FVF in vocal fold abduction and adduction in 30 participants using a linear array transducer (4–10 MHz). Twenty-eight participants met inclusion criteria as healthy subjects for analysis. Mean strain of FVF produced by FVF movement from abduction to adduction was analyzed using 2D speckle-tracking software offline. A SWV ratio ( $[SWV_{\text{adduction}} - SWV_{\text{abduction}}]/SWV_{\text{abduction}}$ ) was developed to test the contractibility of FVF. Statistical analysis included one-way ANOVA to test the difference in mean strain, SWV (adduction and abduction), and SWV ratio among the three age groups; linear regression to analyze correlations of stiffness and movement between the right and left FVF; and intraclass correlation coefficient (ICC) to examine intra- and interobserver reliability in performing shear wave elastography (SWE) of FVF.

**Results**—The 28 healthy participants were divided into 3 age groups (10 of young 20–44 years; 9 of mid-age 45–64 years; and 9 of senior  $\geq 65$  years). The SWV in FVF abduction was higher and the SWV ratio was lower in seniors compared to young participants ( $P < .05$ ). Good to excellent correlation of mean strain and SWV between both FVFs ( $R^2 > 0.89$ ). The reliability of performing SWE of FVF was moderate to excellent.

**Conclusion**—Ultrasound elastography is feasible to assess the stiffness, dynamic movement, and symmetry of adult FVF, and healthy seniors may exhibit increased FVF stiffness.

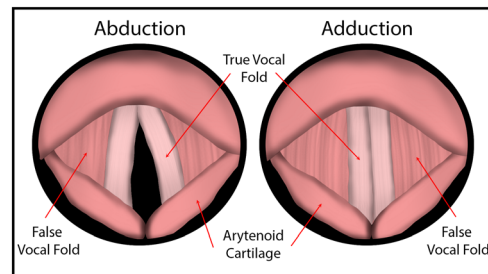
**Key Words**—age; false vocal fold; shear wave elastography; tissue stiffness; ultrasound

The main structural components of the larynx include the thyroid and cricoid cartilages, and thyroarytenoid, vocalis, arytenoid, and cricoarytenoid muscles. These muscles manipulate the tension and shape of the false vocal folds (FVFs) to influence vibration of the true vocal folds, to influence sound waves, allowing for phonation. The true vocal folds are structures that vibrate and oppose each other, which comprise of the vocal ligaments and the overlying mucosa. FVFs are a pair of thick folds comprised of mucous membranes that are located in the supraglottal space in the larynx.<sup>1</sup> The true vocal folds and FVFs are connected to thyroarytenoid and vocalis muscles, respectively, which are both composed of skeletal muscle fibers histologically.<sup>2</sup>

**Figure 1.** Flow chart for participant enrollment.

Observations made to in vitro skeletal muscle tissues has led to a consensus that changes in muscle histology create dynamic responses to mechanical muscle function. Previous studies have proven that skeletal muscles undergo age-related changes over time, including increases in collagen content at the histological level and decreases in type 2 muscle fibers.<sup>3,4</sup> These changes may lead to age-related muscle tissue deterioration as one of causes to develop vocal function disorders in elderly. The term *presbyphonia* refers to various symptoms (eg, increased vocal roughness, shortening in phonation duration, and vocal instability) associated with vocal aging.<sup>5</sup> Histological changes in age-related human skeletal muscles have been assessed and cross-verified using noninvasive imaging modalities, including magnetic resonance imaging<sup>6</sup> and ultrasound shear wave elastography (SWE).<sup>7,8</sup> However, we did not find any report on the age-related change in FVF tissue properties and function using ultrasound elastography during our literature review.

B-mode ultrasonography has proven to be an effective modality to assess airway and laryngeal structures.<sup>9</sup> Using B-mode ultrasonography has clinical values to be an effective strategy for the assessment of functionality and overall health of FVF, and specifically through assessment of tissue morphology and symmetry of the bilateral FVF.<sup>10</sup> Ultrasound imaging is not only beneficial in the sense that it provides a real-time image for motion, but it also reduces the

**Figure 2.** Illustration shows the anatomy of true vocal folds and VFVs.

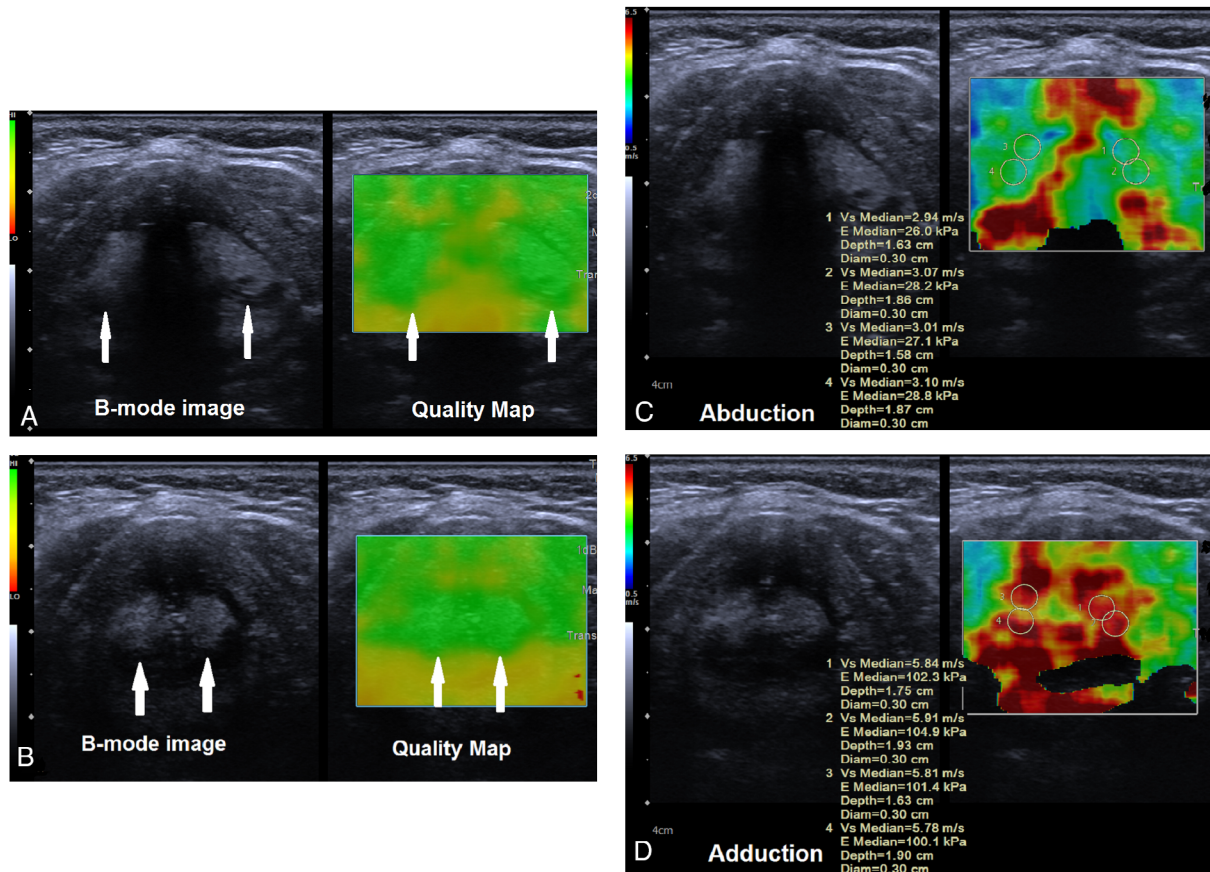
need for more invasive modalities to assess tissue functionality such as invasive transesophageal imaging of the larynx or surgical biopsy for histological assessment of FVF tissue. SWE has been used to evaluate normal mechanical properties (stiffness) of skeletal muscles, and the change in increased passive muscle stiffness with stretched muscles.<sup>11</sup> There are a few reports of using ultrasound elastography (SWE and strain imaging) to assess FVF.<sup>12</sup> We aimed to investigate the feasibility of SWE for evaluation of mechanical properties, function, and symmetry in adult FVF with age.

## Material and Methods

### Participants

The Institutional Review Board at the Rocky Vista University approved the study (IRB# 2019-0088)

**Figure 3. A–D,** Virtual Touch IQ (VTIQ) was used for SWE of FVFs. Shear wave quality map (quality map) is displayed side by side with B-mode image prior to measuring SWV of FVF (white arrow). The quality of SWE is considered valid once homogeneous green appearing in the entire region of FVF in abduction (**A**) and adduction (**B**). Color-coded SWV image of FVF is displayed side by side with B-mode image. Point shear wave elastography (circle region of interest with 0.3 cm in diameter) is used to measure SWV (m/s) in each side of FVF, twice in abduction (**C**) and twice in adduction (**D**). It is clear to note that SWV is low in FVF abduction (FVF relaxation) and high in FVF adduction (FVF contraction).



and all participants provided written informed consent. All adult participants were volunteers recruited in the local community (Figure 1). Participants underwent a self-reported screening questionnaire to assess previous backgrounds of extensive voice training that may impact a normal cord function (such as professional singer or vocal performing artists).

The inclusion criteria included age older than 18 years, good health (based on an annual physical examination), and the ability to sign written informed consent, tolerate supine position, neck extension, perform the Valsalva maneuver, and undergo an ultrasound examination.

While the inclusion criteria for the study exam was broad, including healthy and subjects with potential FVF disease, the exclusion criteria for this analysis of healthy subjects were a history of hoarseness, irritant cough, and vocal fold disease of any kind, thyroid, parathyroid, and cervical spine surgery, tracheostomy, cervical trauma, or neuromuscular disorders (eg, stroke).

#### *Transcutaneous Ultrasound SWE of FVFs*

An Acuson Sequoia ultrasound scanner (Siemens Healthineers) equipped with a 10L4 linear array transducer was used to acquire grayscale images of FVFs. Virtual Touch Tissue Quantification (VTIQ) software installed in the scanner was used to measure

**Figure 4. A–C,** Cine loops of real-time grayscale image of FVFs containing FVF dynamic movement from abduction (**A**) to adduction (**C**) were recorded for offline processing using 2D speckle-tracking software. Ultrasound strain represents the movement and symmetry of right (red dotted and solid lines) and left (cyan dotted and solid lines) FVF. Mean strain is the average of strain produced during 1 cycle of FVF movement from abduction (**A** and **B**, yellow arrow) to adduction (**B** and **C**, red arrow). The notion is that FVF tissue lengthened (**B**, positive strain pointed by the yellow arrow) in FVF abduction and shortened (**B**, negative strain pointed by the red arrow) in FVF adduction.

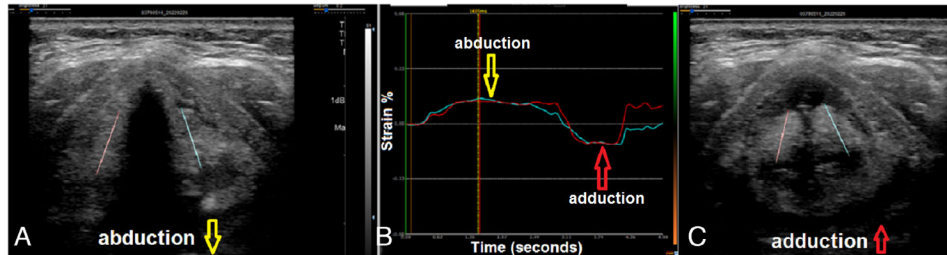


**Table 1.** Shear Wave Elastography of FVFs Among the Three Age Groups

Parameter	Young Age	Mid-Age	Old Age	ANOVA (P)
Number of subjects	10	9	9	
Male/female	5/5	2/7	5/4	
Mean age (years)	25 ± 1	54 ± 8	69 ± 3	<.001
Body mass index (kg/m <sup>2</sup> )	23.3 ± 3.21	23.3 ± 5.02	26.7 ± 3.9	.14
SWV: FVF-abduction (m/s)	3.26 ± 1.0	3.47 ± 1.0	4.06 ± 0.87	.04
SWV: FVF-adduction (m/s)	4.36 ± 1.08	4.56 ± 0.93	4.88 ± 1.12	.32
SWV ratio	0.47 ± 0.37	0.44 ± 0.34	0.22 ± 0.19	.04
FVF mean strain	0.22 ± 0.08	0.21 ± 0.10	0.18 ± 0.07	.33

P value shows the difference in SWV (m/s) in FVFs abduction and adduction among the three age groups tested by one-way ANOVA. SWV ratio is defined by SWV ratio = (SWV<sub>adduction</sub> – SW<sub>abduction</sub>)/SW<sub>abduction</sub>.

**Table 2.** Post Hoc of FVF SWV in Abduction and Adduction Among the Three Age Groups

Post Hoc <sup>a</sup>	Young Age vs Mid-Age	Young Age vs Old Age	Mid-Age vs Old Age
SWV: FVF abduction	0.21, –0.54 to 0.96, 0.78 <sup>b</sup>	0.79, 0.04 to 1.54, 0.04	0.58, –0.19 to 1.35, 0.18
SWV: FVF adduction	0.20, –0.62 to 1.02, 0.83	0.52, –0.30 to 1.34, 0.29	0.32, –0.52 to 1.16, 0.63
FVF SWV ratio	–0.03, –0.27 to 0.21, 0.95	0.25, –0.49 to 0.01, 0.04	–0.22, –0.47 to 0.03, 0.09
FVF mean strain	–0.01, –0.08 to 0.06, 0.93	–0.04, –0.11 to 0.03, 0.32	–0.03, –0.10 to 0.04, 0.54

SWV ratio is calculated by SWV ratio = (SWV<sub>adduction</sub> – SW<sub>abduction</sub>)/SW<sub>abduction</sub>.

<sup>a</sup>Tukey HSD (honestly significant difference) post hoc test, to exam that groups significantly differ from which others and provide 95% confidence intervals around the differences between the groups.

<sup>b</sup>Difference, 95% confidence interval, P value based on post hoc analysis.

the shear wave velocity (SWV) within the bilateral FVFs in both abduction and adduction.

There was no specific preparation prior to the ultrasound scan. The participants were placed in the supine position. A small pillow was placed under the neck to maintain mild neck extension. The transducer was placed transversely on the anterior mid neck where the true vocal folds and FVFs are located posterior to the thyroid cartilage (Figure 2). Transmission gel was applied between the skin surface of the anterior neck

and the transducer, a particularly relevant consideration when the angle of the thyroid cartilage was sharp, such as in the male participants examined. Machine pre-setting for thyroid ultrasound was used. We started with B-mode image to evaluate laryngeal morphologic characteristics and observe the movement of the FVFs to guide SWE of FVF. Then, VTIQ mode was activated to measure the SWV, representing the mechanical properties (stiffness) of bilateral FVFs, in both abduction (at the end of inspiration during a normal breath) and



adduction (as performing maximal Valsalva maneuver) without phonation or swallowing. A shear wave quality map generated by the VTIQ software was used to ensure the quality of shear wave speed estimation before measuring quantitative SWV values. The shear wave quality was considered valid when a homogeneous green area appeared throughout the region of the FVFs (Figure 3, A and B). Images with regional absence of green in the FVFs within the quality map were considered poor quality and were excluded from the analysis. Quantitative SWV values were then measured within color-coded SWV maps where high-quality SWE results appeared using point SWE (a circle region of interest with 0.3 cm in diameter). A total of 4 SWV measurements were obtained in each side of FVF. Two investigators (L.C. and J.O., underwent 2 years of training in general ultrasound and 40 hours of training in SWE) performed SWE of FVFs twice on each participant in FVF abduction (Figure 3C) and again in FVF adduction (Figure 3D), with an interval of 1 minute, in all participants. For assessing the function of FVFs movement, we developed an SWV ratio defined as  $([SWV_{\text{adduction}} - SW_{\text{abduction}}]/SW_{\text{abduction}})$  for assessing FVF contraction from abduction to adduction. The average of 4 SWV ratio measurements was used for analysis.

To test intraobserver repeatability, each investigator measured SWV of FVF (abduction and adduction) two times on each of 10 participants. To test interobserver reproducibility, 2 investigators measured SWV of the FVF on the same 10 participants separately. The data were analyzed offline.

### Ultrasound Strain Imaging of FVFs

Using the same linear ultrasound transducer, 5-second gray scale image cine loops consisting of real-time ultrasound data of FVF movement from abduction to adduction were stored for offline processing. Machine settings for ultrasound strain imaging included image frame rate >40 frames per second, off speckle reduction function, single image focus, and harmonic imaging. All recorded cine loops were recorded in Digital Imaging and Communications in Medicine (DICOM) format and transferred to a PC for offline image processing. A 2D speckle-tracking

**Figure 5. A–C,** Scatter plots show good correlations of SWV (m/s) between the right and left FVFs stiffness in FVF abduction (**A**,  $R^2 = 0.948$ ) and in adduction (**B**,  $R^2 = 0.895$ ). A strong correlation between the right and left FVF movement assessed by the mean strain is also demonstrated by linear regression (**C**,  $R^2 = 0.984$ ).

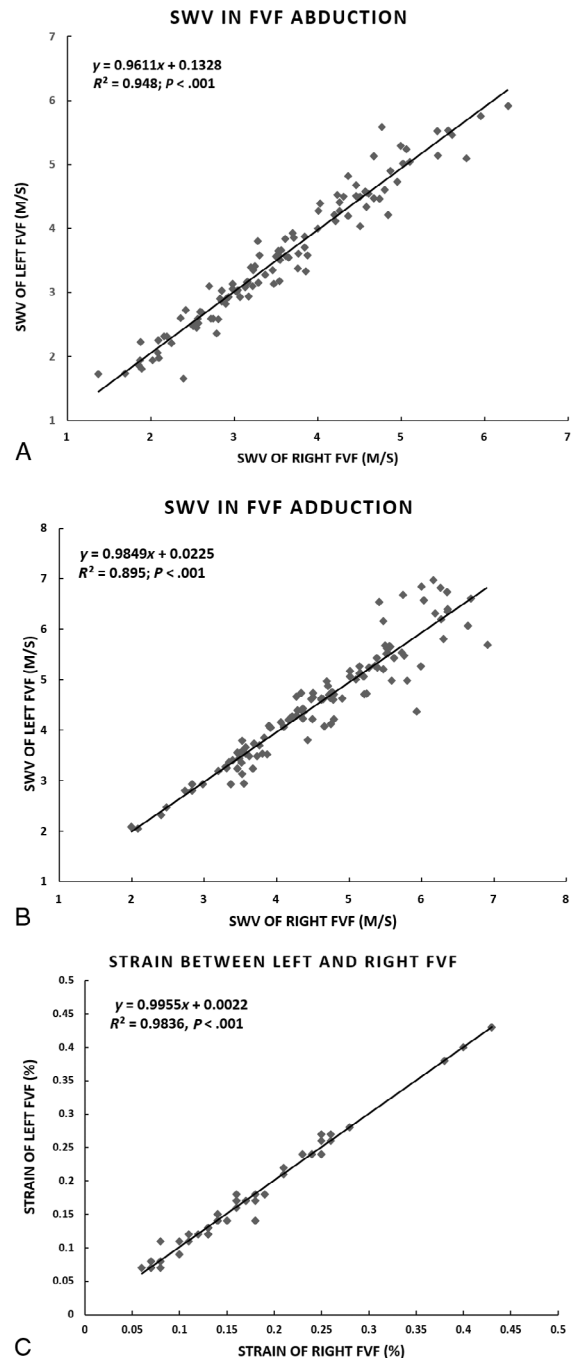


**Table 3.** Intra- and Interobserver Reliability in Measuring SWV of the FVF

Average Measures	Intraclass Correlation <sup>a</sup>	95% Confidence Interval		F Test with True Value 0	
		Lower Bound	Upper Bound	Value	Sig
Operator 1:operator 1 -FVF adduction	0.92	0.85	0.96	12.86	<.001
Operator 2:operator 2 -FVF adduction	0.82	0.67	0.91	5.64	<.001
Operator 1:operator 2 -FVF adduction	0.75	0.65	0.87	3.99	<.001
Operator 1:operator 1 -FVF abduction	0.89	0.79	0.94	9.19	<.001
Operator 2:operator 2 -FVF abduction	0.85	0.72	0.92	6.83	<.001
Operator 1:operator 2 -FVF abduction	0.87	0.77	0.93	7.66	<.001

<sup>a</sup>ICC, intraclass correlation coefficient. Interobserver reliability test: measurements performed by the operator 1 to measurements performed by the operator 2 on the same patients separately; intraobserver reliability tests: measurement 1 to measurement 2 performed on the same patients by a single operator. Operator 1 and operator 2 had 2 years training in performing neck and soft tissue ultrasound and 40 hours training for performing shear wave elastography.

software (EchoInsight, Epsilon Imaging, Ann Arbor, MI, USA) was used to estimate mean strain of each FVF produced during FVF movement from abduction to adduction.<sup>13</sup> Mean strain of FVF is the average absolute strain produced from FVF abduction to adduction (Figure 4).

### Statistical Analyses

The variability of the mean strain, SWV, and SWV ratio within FVFs and the ages, and body mass index of the participants was expressed as mean  $\pm$  standard deviation. The difference in the SWV between the right and left FVFs and between FVFs in adduction and abduction were analyzed by a paired *t* test. The difference in SWV, SWV ratio, and mean strain among the three age groups were tested using one-way ANOVA and post hoc. The correlation of mean strain, and SWV between the right and left FVFs was tested by the linear regression. Intra- and interobserver reliability was analyzed using intraclass correlation coefficient (ICC).  $P < .05$  considered statistically significant. Statistical analyses were performed with commercial software (SPSS, Version 27.0, SPSS, Intel).

## Results

We initially recruited 30 participants for ultrasound elastography measurements from February to April

2021. The current study consists of the analysis of 28 healthy subjects from this population. Two participants (1 participant with hoarseness and 1 underwent total thyroidectomy) were excluded from the analysis (Figure 1). All data from the healthy subjects used in this analysis including mean strain, SWV, SWV ratio of FVF, and demographic information of participants are listed in Table 1.

The difference in SWV in FVF abduction and SWV ratio were significant between senior and young age group ( $P < .05$ ). SWV of FVF was higher and SWV ratio was lower in seniors compared to those in young participants. Differences in mean strain and SWV in FVF adduction were not significant among the three age groups ( $P > .05$ ; Table 2). Strong correlations in SWV between the right and left FVF in FVF abduction ( $R^2 = 0.948$ ; Figure 5A), adduction ( $R^2 = 0.895$ ; Figure 5B), and mean strain ( $R^2 = 0.984$ ; Figure 5C) were observed.

Intraobserver repeatability and interobserver reproducibility were moderate to excellent (ICC = 0.75–0.92; Table 3).

## Discussion

Yet, imaging true vocal folds and FVFs is not well established although approximately 10 to 30% of the population are affected by problems of their voice in

their lifetime, professional speakers or singers up to 50%.<sup>14</sup> Patient management can be improved by introducing a reliable, noninvasive method for the assessment of the change in vocal folds function. Our study showed the effectiveness of SWE and ultrasound strain imaging for assessing FVF stiffness and function that may change with age. This may eliminate the need for invasive procedures (such as endoscopic vocal cord biopsies or endoscopic ultrasonography) when assessing changes in vocal fold function in elderly.<sup>15,16</sup> To our knowledge, this is the first report of ultrasound elastography to quantify changes in the FVFs stiffness (in adduction and abduction) and symmetry associated with aging. Attempts were made to compare the varying muscle fiber tensions in healthy individuals across different age groups in the hope of correlating the influence of age on the FVF stiffness and function.<sup>15,16</sup> Our results highlight the differences in ultrasound strain and SWV in varying states of FVF movement, associated with decreased elasticity in progressively older age groups.

There was no significant difference in SWV between the right and left FVF in the same age groups. The difference in SWV between FVF abduction and adduction in each age group was significant (Table 1). SWV measured in FVF abduction, occurring with FVF-associated muscle full relaxation, was lower than in FVF adduction, occurring with FVF-associated muscle maximal contraction. These results are consistent with previous data showing changes in muscle stiffness with variable degrees of active or passive muscle tension measured by SWV.<sup>9</sup>

There was a statistically significant difference in the SWV of FVFs between the senior and young age groups in FVF abduction ( $P < .05$ ) (Table 1). Mean SWV in seniors was higher than participants in young age group (4.06 versus 3.26 m/s). This suggests that age-related changes in FVF may be important in establishing reference ranges for future studies or clinical applications. These data may also serve as an initial reference for applications assessing muscle stiffness changes from other disorders when applied to different age groups, since FVF stiffness increases with age. Differences in FVF stiffness measured by SWV between the young and mid-age groups, and participants between the mid-age and senior age groups were not significant ( $P > .05$ ) (Table 2). There was no significant difference in the mean SWV representing mechanical properties of FVFs between all groups in FVF adduction ( $P > .05$ )

(Table 1). Since this is the first observation of age-related changes in measured FVF stiffness by ultrasound elastography, larger studies may be needed to detect more subtle changes. There are additional factors that must be considered when assessing FVF stiffness. For example, underlying tissue stiffness changes may be compensated for by the contractibility of FVF and associated muscles in healthy seniors. Another factor is the difficulty in normalizing a “maximal contraction” when patients perform the Valsalva maneuver for measuring SWV in the FVF adducted (contraction). There are data to suggest that varying the force (strength) of voluntary muscle tension placed on the FVF may only lead to insignificant differences in evaluating the muscle stiffness in contracted muscles.<sup>7</sup> Given the complexity of the anatomy and mechanical changes our findings suggest that the FVF tissue properties should be evaluated in both the abducted state and adducted state to help account for changes in FVF stiffness in different stages of voluntary muscle contraction and relaxation.

The difference in the developed SWV ratio (a ratio of the difference in SWV between the FVF in abduction and adduction to FVF abduction) was also significant between the young age and senior groups (Table 1). The SWV ratio in seniors was substantially lower than young age participants (0.22 versus 0.47,  $P = .04$ ) suggesting that the contractibility of FVF decreased with age. This may help explain clinical symptoms in the development of age-related vocal disorders.<sup>5</sup> These results may be helpful as an important reference when evaluating diminished function of vocal folds caused by thyroid and parathyroid surgery, as well as other neuromuscular disorders (eg, Parkinson disease).<sup>17–19</sup> Our ultrasound elastography age-dependent findings for SWV and SWV ratio are consistent with observations by others that age-related FVF local tissue degeneration may lead to an increase of stiffness and decrease of function of FVF.<sup>2,3</sup>

Having symmetry of FVF mechanical properties is essential for maintaining normal function of voice production, breathing, and swallowing.<sup>10</sup> In this study with healthy subjects, we found SWV and mean strain of bilateral FVF demonstrated strong correlations between sides of the FVFs in abduction, in adduction, and during movement from abduction to adduction (Table 3). Asymmetry may detect unilateral FVF movement abnormalities caused by either primary muscle fiber pathology or secondary to nerve damage in a neck surgery.

Previous studies have shown that a poor correlation in SWV between opposite FVF sides may indicate asymmetric tissue mechanics in patients with unilateral nerve injury or unilateral vocal cord paralysis.<sup>12,19</sup>

An important additional observation, we successfully performed ultrasound strain and SWE of FVF in all 28 subjects, differing from previous observations that soft-tissue-air interface and calcified thyroid cartilage in adults precluded the visualization of laryngeal structures and muscles.<sup>20</sup> Additionally, we demonstrated good to excellent intraobserver and interobserver reproducibility in measuring SWV of the FVFs performed by two junior operators (ICC >0.75;  $P < .001$ ) (Table 3). These two observations suggest that this technique might be more approachable for future study and clinical adoption than previously realized. There are advantages of using ultrasound strain imaging to assess FVF compared with acoustic radiation force impulse (ARFI)-based SWE. Ultrasound strain (fraction) represents the relation between the altered tissue lengths (tissue shortening in contraction or deformation under compression) to its initial length for quantifying the tissue movement or deformation associated with tissue function and stiffness.<sup>12</sup> The locations of ultrasound speckles (kernel) in sequence of FVF grayscale real-time cine loops change following FVF movement from abduction to adduction, which can be processed (tracked) using 2D speckle-tracking software frame by frame and displayed using a strain curve (Figure 4).<sup>12</sup> SWE only measures the stiffness of FVF in abduction and adduction on static images.<sup>13</sup> Furthermore, tissue strain can be processed based on DICOM ultrasound cine loops recorded from any ultrasound scanners (portable or stationary) using an offline 2D speckle-tracking software. To date, however, ARFI-based SWE still require a dedicated high-end ultrasound scanner.

There were limitations to this study, principally related to the relatively small number of participants enrolled in the study. In addition, our study was not designed to detect pathological changes that may impact the functionality of the FVFs. We anticipate that the value of the SWV of FVFs may differ in a population with laryngeal disorders (eg, vocal fold impairment). Nevertheless, detecting age-related changes in the general population will be important in establishing reference ranges for ultrasound elastography to be used in detecting FVF pathology. Disorders that lead to symmetrical FVF

pathology may need age-dependent references to be used clinically. Another measurement factor that needs to be considered is that each participant had differing levels of FVF contraction when performing the Valsalva maneuver, and thus muscle tension. These differences may lead to variation in the SWV. More work is required to understand how to interpret ultrasound elastography in FVF disorders, such as benchmarking with other imaging modalities, such as laryngeal magnetic resonance or electromyography. Furthermore, other patient life style and populations must be tested, such as history of smoking or smokeless tobacco use and vocal performing artists, to understand the breadth of measurement for ultrasound elastography FVF results in health, different life style, and disease. The reproducibility of performing ultrasound strain of FVF over time was not conducted in the study. However, good intraobserver repeatability has been previously reported.<sup>12</sup>

In conclusion, our study results suggest that SWE is feasible for noninvasive assessment of stiffness, function, and symmetry of the FVFs through a transcutaneous approach. Additionally, we detected age-related changes in an increase of FVF stiffness and decrease of FVF contractibility in seniors compared with young age participants in this healthy population without known vocal fold disorders. Bilateral FVF symmetry is demonstrated by close correlations of SWV in abduction and adduction representing FVF tissue stiffness, and mean strain representing FVF function in healthy adults. Additional study using ultrasound elastography to further assess age-related and pathologic changes in true vocal folds and FVFs disorders is warranted.

## References

1. Moon J, Alipour F. Muscular anatomy of the human ventricular folds. *Ann Otol Rhinol Laryngol* 2013; 122:561–567.
2. Thomas LB, Harrison AL, Stemple JC. Aging thyroarytenoid and limb skeletal muscle: lessons in contrast. *J Voice* 2008; 22: 430–450.
3. Larsson L, Degens H, Li MS, et al. Sarcopenia: aging-related loss of muscle mass and function. *Physiol Rev* 2019; 99:427–511.
4. Goodpaster BH, Park SW, Harris TB, et al. The loss of skeletal muscle strength, mass, and quality in older adults: the health, aging and body composition study. *J Gerontol A Biol Sci Med Sci* 2006; 61:1059–1064.



5. Karbiener M, Jarvis JC, Parkins JD, et al. Reversing age related changes of the laryngeal muscles by chronic electrostimulation of the recurrent laryngeal nerve. *PLoS One* 2016; 11:e0167367. <https://doi.org/10.1371/journal.pone.0167367>.
6. Debemard L, Robert L, Charleux F, Bensamoun SF. Analysis of thigh muscle stiffness from childhood to adulthood using magnetic resonance elastography (MRE) technique. *Clin Biomech* 2011; 26:836–840.
7. Eby SF, Cloud BA, Brandenburg JE, et al. Shear wave elastography of passive skeletal muscle stiffness: influences of sex and age throughout adulthood. *Clin biomech* 2015; 30:22–27.
8. Maisetti O, Hug F, Bouillard K, Nordez A. Characterization of passive elastic properties of the human medial gastrocnemius muscle belly using supersonic shear imaging. *J Biomech* 2012; 45:978–984.
9. Singh M, Chin KJ, Chan VWS, Wong DT, Prasad GA, Yu E. Use of sonography for airway assessment: an observational study. *J Ultrasound Med* 2010; 29:79–85.
10. Wang CP, Chen TC, Lou PJ, et al. Neck ultrasonography for the evaluation of the etiology of adult unilateral vocal fold paralysis. *Head Neck* 2012; 34:643–648.
11. Su E, Hamilton C, Tawfik DS, et al. Laryngeal ultrasound detects vocal fold immobility in adults. *J Ultrasound Med* Published online November 27, 2021. <https://doi.org/10.1002/jum.15884>.
12. Gao J, Xia CX, Zhu Q, Hamilton J, Min R. Ultrasound strain imaging in assessment of false vocal folds in adults: a feasibility study. *Clin Imaging* 2018; 51:292–299.
13. Gao J, Zhu Q, Xia CX, Shin J, Shih G, Min R. Shear wave elastography to assess false vocal folds in healthy adults: a feasibility study. *J Ultrasound Med* 2018; 37:2537–2544.
14. Martins RHG, Pessin ABB, Nassib DJ, et al. Aging voice and the laryngeal muscle atrophy. *Laryngology* 2015; 125:2518–2521. <https://doi.org/10.1002/lary.25398>.
15. Lamprecht R, Maghzinajafabadi M, Döllinger M, Semmler M, Sutor A. Elastography of vocal folds. *J Phys Conf Ser* 2019; 1379:012016.
16. Baken RJ. The aged voice: a new hypothesis. *J Voice* 2005; 19:317–325.
17. Anathkrishnan R, Gopalakrishnan S, Elangovan S. Use of ultrasound to assess superior and recurrent laryngeal nerve function immediately after thyroid surgery. *Anesthesia* 2012; 67:301–302.
18. Wong KP, Woo JW, Youn YK, Chow FCL, Lee KE, Lang BHH. The importance of sonographic landmarks by transcutaneous laryngeal ultrasonography in post-thyroidectomy vocal cord assessment. *Surgery* 2014; 156:1590–1597.
19. Kumar A, Sinha C, Kumar A, et al. Assessment of functionality of vocal cords using ultrasound before and after thyroid surgery: an observational study. *Indian J Anaesth* 2018; 62:599–602. [https://doi.org/10.4103/ija.IJA\\_197\\_18](https://doi.org/10.4103/ija.IJA_197_18).
20. Beale T, Twigg VM, Horta M, Morley S. High-resolution laryngeal US: imaging technique, normal anatomy, and spectrum of disease. *RadioGraphics* 2020; 40:775–790.